CRAWLEY, A. F. & FABIAN, D. J. (1966). *J. Inst. Met.* **94**, 39.
DISMUKES, J. P., EKSTROM, L. & PAFF, R. J. (1964). *J. Phys. Chem.* **68**, 3021, 3025.
DOYLE, N. J., HULM, J. K., JONES, C. K., MILLER, R. C. & TAYLOR, A. (1968). *Phys. Letters*, **26A**, 604.
ELLWOOD, E. C. (1951). *J. Inst. Metals*, **80**, 217.
HANSEN, M. (1958). *Constitution of Binary Alloys*, pp. 590–592. New York: McGraw-Hill.
HAUFFE, K. (1966). *Reaktionen in und an festen Stoffen*, p. 483. Berlin: Springer-Verlag.
HELFRICH, W. J. & DODD, R. A. (1962). *Trans. Met. Soc. AIME*, **224**, 757.
HELFRICH, W. J. & DODD, R. A. (1963). *Acta Met.* **11**, 982.
HELFRICH, W. J. & DODD, R. A. (1964). *Acta Met.* **12**, 667.
HUME-ROTHERY, W., RAYNOR, G. V., REYNOLDS, P. W. & PACKER, H. K. (1940). *J. Inst. Metals*, **66**, 209.
JONES, R. O. & OWEN, C. A. (1953). *J. Inst. Metals*, **82**, 445.
LEE, J. A. & RAYNOR, G. V. (1954). *Proc. Phys. Soc.* (13), **67**, 737.
MACIOLEK, R. B., MULLENDORE, J. A. & DODD, R. A. (1967). *Acta Met.* **15**, 259.
OVSIENKO, D. E. (1968). *Growth and Imperfections of Metallic Crystals*, pp. 131, 143, 144, 145, 146. New York: Consultants Bureau.
OWEN, E. A. & ROBERTS, E. A. O'D. (1952). *J. Inst. Metals*, **81**, 479.
RHINES, F. N. (1956). *Phase Diagrams in Metallurgy. Their Development and Application*. pp. 24, 25, 85. New York: McGraw-Hill.
RIDER, J. G. & RONEY, P. L. (1962). *J. Inst. Met.* **91**, 328.
RUEDL, E., DELAVIGNETTE, P. & AMELINCKX, S. (1962). *J. Nucl. Mat.* **6**, 46.
STRAUMANIS, M. E. (1949). *Acta Cryst.* **2**, 82.
STRAUMANIS, M. E. (1953). *Phys. Rev.* **92**, 1155.
STRAUMANIS, M. E. (1954). *Phys. Rev.* **95**, 566.
STRAUMANIS, M. E. (1963). In *Encyclopedia of X-rays and Gamma Rays*, pp. 733, 700. New York: Reinhold.
STRAUMANIS, M. E. & IEVIŅŠ, A. (1959). *The Precision Determination of Lattice Constants by the Asymmetric Method*. Portsmouth, Ohio: Goodyear Atomic Corp.
STRAUMANIS, M. E. & LI, H. W. (1960). *Z. anorg. allg. Chem.* **305**, 143.
STRAUMANIS, M. E. & RIAD, S. M. (1965). *Trans. Met. Soc. AIME*, **233**, 964.
WEIBKE, F. & EGGERS, H. (1934). *Z. anorg. Chem.* **220**, 273.

Acta Cryst. (1969). A**25**, 682

X-ray Diffraction from a Crystal Containing Isolated Imperfections

BY MASAO KURIYAMA

National Bureau of Standards, Institute for Materials Research, Washington, D.C. 20234, *U.S.A.*

(*Received* 20 *December* 1968)

The X-ray scattering amplitude of a crystal containing isolated imperfections is expressed in terms of the Fourier transform of the atomic displacement vectors. The amplitude contains only the local properties of the imperfections which are 'seen' by the incident beam of a finite size. Disruption of the Borrmann transmitted (or diffracted) beam, narrowing of the dynamical diffraction range and 'diffuse' scattering caused by dynamically diffracted X-rays are some of the results obtained from the calculated amplitude. Black, white and black-white images in topographs are explained by the present theory. Image contrast is also discussed in terms of the thickness of the crystal.

1. Introduction

Recent interest in X-ray diffraction from a single crystal has been centred on the fine structure in a Laue spot. This fine structure is closely related to imperfections in crystals. The techniques of X-ray topography 'magnify' at high resolution a Laue spot from a large portion of a crystal.

In the X-ray topographs obtained from an imperfect crystal, one observes black and white images superimposed on a background. For a *thin* crystal where the product of the linear absorption coefficient μ and the thickness L is less than 1, defects may appear as black (stronger intensity) images accompanied by a faint anomalous transmission (or diffraction) beam trace. For *intermediate* thickness where $1<\mu L<10$, the topographs show primarily white images. Black images also appear as well as black-white contrast images. Usually one should expect complicated patterns for these cases. For a *thick* crystal ($\mu L>10$), the Borrmann (anomalous transmission) effect (Borrmann, 1941, 1950) becomes dominant and is accompanied by white images of good contrast. Black images or non-uniform intensity distribution may still be observed in the topographs. The above qualitative description of images is based on casual observation of topographs. More complicated patterns including interference effects, *etc.* are also observed.

The primary objective of this paper is to present some of the explanations for the formation of the images mentioned above, by use of a previously formulated general theory of scattering from an imperfect crystal (Kuriyama, 1967*a*, 1968*b*). This theory has been derived with a large degree of rigor. Wherever approx-

imations were introduced, the probable loss in accuracy has been estimated mathematically. Physically speaking these approximations are very good. To employ the theory simply, however, it is convenient to relax the rigor in mathematics, especially for the description of atomic displacements.

Since the characteristics of atomic displacements vary, depending on the type of imperfection, it is very difficult to obtain the explicit form of the X-ray scattering amplitude generally valid for a crystal so that one could make unequivocal deductions on any given imperfections. One can, however, calculate the scattering amplitude for various defects, case by case, if the atomic displacements are given so that the geometrical structure factor can be calculated numerically. In this way one may be able to obtain the accurate scattering amplitude for each type of defect (provided that the atomic displacements can always be given) since the theoretical formulation of the scattering amplitude is quite accurate. However, in the process of numerical calculations there exists real danger that one tends to lose sight of the general features of the scattering processes. Since our interest is a basic understanding of the diffraction processes in an imperfect crystal, it is best to preserve the generality of the resultant scattering amplitude regardless of the type of defect. The basic diffraction processes will be discussed separately from the effect due to the atomic displacements which mostly appears as a geometrical factor. At the expense of mathematical rigor, we shall introduce some physical assumptions for describing the physical characteristics of imperfections.

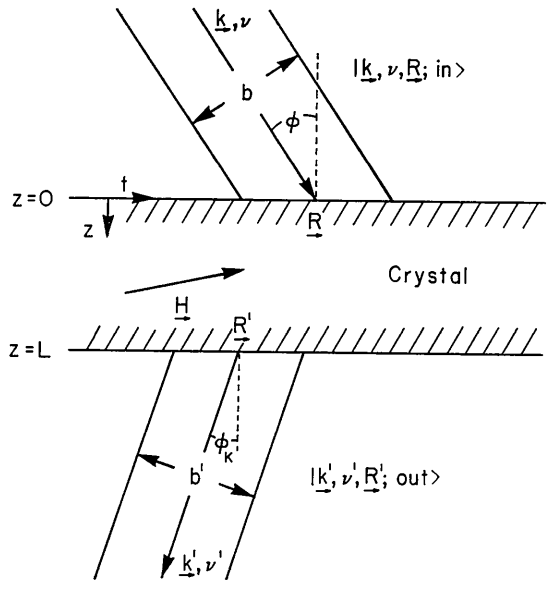

Fig. 1. Beam geometry for Laue transmission. The incident beam defines the initial photon state $|\mathbf{k}, \nu, \mathbf{R}; \text{in} >$ and the scattered beam defines the final photon state $|\mathbf{k}', \nu', \mathbf{R}'; \text{out} >$. When $\mathbf{k}' = \mathbf{k} + \mathbf{K}$ with $\mathbf{K} = \mathbf{O}$ and $\mathbf{H}$, the final state gives the photons scattered in the transmitted ($\mathbf{K} = \mathbf{O}$) and the Bragg diffracted ($\mathbf{K} = \mathbf{H}$) directions with respect to the perfect reference crystal. Generally, $\mathbf{k}'$ is arbitrary.

Since we are interested in topographic images, the scattering amplitude by an incident beam of finite size will be studied. Imperfection effects on the diffracted beams are here treated as caused solely by the state of the crystal, *not* by the state of the incident beam. Therefore, we shall here minimize the effect due to the intrinsic momentum (wave number) dispersion in the incident beam.

It must be admitted that in any practical experiment a finite dispersion is inescapable. For instance, if the slit size is reduced below about 10^{-5} m, properties inherent in wave optics introduce significant dispersion, which cannot be neglected in dynamical diffraction. Nevertheless the basic premise of the theory in neglecting intrinsic dispersion is held to be valid, even if better radiation sources – such as X-ray lasers – are not yet available.

2. General expression of the scattering amplitude

In this paper we shall deal with an imperfect crystal plate, on which an X-ray beam of finite lateral size is incident, nearly satisfying a single Bragg reflection condition. The incident X-ray beam having lateral widths a and b, characterized by momentum $\mathbf{k}$, energy $k = |\mathbf{k}| = 2\pi/\lambda$ (with $\hbar = c = 1$) and polarization direction $\mathbf{v}$, impinges at $\mathbf{R}$ on a crystal surface with the incident angle φ. We call this crystal surface the entrance surface. The incident position $\mathbf{R}$ merely denotes the center position of the incident beam.

Since a single Bragg reflection condition is assumed for the momentum $\mathbf{k}$ of the incident X-rays, there can be found only one reciprocal lattice vector $\mathbf{H}$ such that the Bragg condition $|\mathbf{k}| = |\mathbf{k} + \mathbf{H}|$ is approximately satisfied. Reciprocal lattice vectors are defined in the perfect reference crystal and denoted in general by $\mathbf{K}$. The perfect reference crystal is an imaginary crystal which is obtained by putting all atoms of a given type at ideally periodical lattice sites.

Any scattered beam, being also finite in its lateral directions, emerges from another crystal surface at $\mathbf{R}'$ with the angle $\varphi_{\mathbf{K}}$ measured from the normal of the surface, having momentum $\mathbf{k}'$, energy k' and polarization direction $\mathbf{v}'$. This surface may be called the exit surface. This beam geometry implies the Laue geometry as shown in Fig. 1. When one of the scattered beams emerges from the entrance surface the Bragg geometry is achieved. In this paper we consider the Laue geometry explicitly.

To obtain the expression for the scattering amplitude we introduce the x and y axes on the X-ray entrance surface which is of infinite extent, and the z axis in the direction of the crystal thickness L. The exit surface is given by $z = L$. We also describe a projection of a vector onto the crystal surface by a subscript t.

The incident X-ray beam gives a photon in the initial state described by $|\mathbf{k}, \nu, \mathbf{R}; \text{in} >$, and the scattered beam

corresponds to a photon in a final state $|\mathbf{k}', \nu', \mathbf{R}'; \text{out}>$. When the crystal is perfect, the possible final states are given by $\mathbf{k}'=\mathbf{k}+\mathbf{K}$ with $\mathbf{K}=\mathbf{0}$ and $\mathbf{H}$. The direction of the $\mathbf{k}'$ is called the transmitted direction when $\mathbf{K}=\mathbf{0}$, and is called the Bragg diffracted direction when $\mathbf{K}=\mathbf{H}$. When the crystal is imperfect, the X-rays are diffracted not only in those directions, but in all directions. In other words, it is possible to have any value for $\mathbf{k}'$ specifying the final state. In reality, however, the X-rays of an observable intensity are usually scattered from a crystal in an angular range around those two directions (Kuriyama, 1968*a*). It is therefore practical to describe the direction of the momentum in the final state by the deviations, supposedly being of a small amount, from the two directions in the following way:

$$\mathbf{k}_t'=\mathbf{k}_t+\xi_t^{\mathbf{0}} \text{ for the transmitted direction} \tag{2·1}$$

and

$$\mathbf{k}_t'=\mathbf{k}_t+\mathbf{H}_t+\xi_t^{\mathbf{H}} \text{ for the Bragg diffracted direction} . \tag{2·2}$$

The scattering amplitude for an X-ray beam of finite size coming into a crystal is now given by the S-matrix for a photon in the wave packet $|\mathbf{k}, \nu, \mathbf{R}; \text{in}>$ to make a transition to the state $|\mathbf{k}', \nu', \mathbf{R}'; \text{out}>$, the crystal remaining in its ground state (Ashkin & Kuriyama, 1966; Kuriyama, 1967*a*). The scattering amplitude for an incident beam of a given shape has been calculated in a previous paper (Kuriyama, 1968*b*). To reproduce that result we introduce the following functions:

$$T(k',k)=\frac{\cos\varphi\cos\varphi_K}{(2\pi)^2}\frac{1}{2k}\delta(k-k') \quad \text{(elastic scattering condition)} \tag{2·3}$$

$$Q(\mathbf{k}_t; i)=[\alpha_i(\mathbf{k}_t)+K_z+k_z'(\mathbf{k}_t)]F_{\mathbf{K}}^{(2)}(\mathbf{k}_t; i) \tag{2·4}$$

$$G_{ij}(\mathbf{K}0;\xi^{\mathbf{K}})=v(\xi^{\mathbf{K}})\,[F_{\mathbf{K}}^{(1)}(\mathbf{k}_t';j)F_{\mathbf{0}}^{(2)}(\mathbf{k}_t;i)+F_{\mathbf{K}-\mathbf{H}}^{(1)}(k_t';j)F_{\mathbf{H}}^{(2)}(\mathbf{k}_t;i)] \tag{2·5}$$

$$G_{ij}(\mathbf{K}+;\xi^{\mathbf{K}})=v(\xi^{\mathbf{K}}+\mathbf{H})F_{\mathbf{K}-\mathbf{H}}^{(1)}(\mathbf{k}_t';j)F_{\mathbf{0}}^{(2)}(\mathbf{k}_t;i) \tag{2·6}$$

$$G_{ij}(\mathbf{K}-;\xi^{\mathbf{K}})=v(\xi^{\mathbf{K}}-\mathbf{H})F_{\mathbf{K}}^{(1)}(\mathbf{k}_t';j)F_{\mathbf{H}}^{(2)}(\mathbf{k}_t;i) , \tag{2·7}$$

where $F_{\mathbf{K}}^{(1)}(\mathbf{k}_t';j)$ and $F_{\mathbf{K}}^{(2)}(\mathbf{k}_t;i)$ are called the *dynamical field functions* in the final and the initial state, respectively, and α_i is the solution to the dispersion equation with the fixed $\mathbf{k}_t$ for the initial state and the explicit forms of those quantities are given in the Appendix. The dynamical field function $F_{\mathbf{K}}^{(2)}(\mathbf{k}_t;i)$ gives the electric field intensity of radiation outside the crystal in the dynamical theory. The quantities $v(\xi^{\mathbf{K}})$ and $v(\xi^{\mathbf{K}}\pm\mathbf{H})$ are derived from a double Fourier transform $\gamma(\mathbf{k}_1,\mathbf{k}_2;\omega)$ of the polarizability of 'atomic' electrons in the unit cell (Kuriyama, 1967*a*) by the relation

$$v(\mathbf{k}_1-\mathbf{k}_2)\simeq\gamma(\mathbf{k}_1,\mathbf{k}_2;\omega) . \tag{2·8}$$

In (2·5)–(2·7) we have also introduced a vector $\xi^{\mathbf{K}}$ whose t-components are given by equations (2·1) and (2·2). Its z-component is defined by the solutions of the dispersion equation for the final state (see the Appendix):

$$\xi_z^{\mathbf{K}}=\beta_j^{\mathbf{K}}(\mathbf{k}_t')-K_z-\alpha_i(\mathbf{k}_t) . \tag{2·9}$$

For simplicity we also use the notation

$$\beta_j=\beta_j^{\mathbf{K}}(\mathbf{k}_t')-K_z . \tag{2·10}$$

The quantity β_j is given in the Appendix, not as a function of $\xi_t^{\mathbf{K}}$, but for practical reasons as a function of the quantity $\eta_{\mathbf{K}}$, which describes the deviation of the observation direction, $\mathbf{k}_t'$, from the Bragg condition. The scattering amplitude for a finite X-ray beam incident on an imperfect crystal can now be written (Kuriyama, 1968*b*), with ν and ν' disregarded,

$$\begin{aligned}\langle\mathbf{k}', \mathbf{R}'; \text{out}|\mathbf{k}, \mathbf{R}; \text{in}\rangle=\langle\mathbf{k}', \mathbf{R}'|S|\mathbf{k}, \mathbf{R}\rangle=T(k',k)\,(ab/\\ \times\cos\varphi_K)\,\Sigma\,\delta(\mathbf{R}', \mathbf{R}; i)Q(\mathbf{k}_t; i)\times\exp\,[iL\{\alpha_i(\mathbf{k}_t)\\ +K_z-k_z'(\mathbf{k}_t)\}]+iT(k',k)\sum_{ij}[\Delta g(\xi^{\mathbf{K}};\mathscr{V})G_{ij}(\mathbf{K}0;\xi^{\mathbf{K}})\\ +\Delta g(\xi^{\mathbf{K}}+\mathbf{H};\mathscr{V})G_{ij}(\mathbf{K}+;\xi^{K})+\Delta g(\xi^{K}-\mathbf{H};\mathscr{V})G_{ij}\\ \times(\mathbf{K}-;\xi^{K})]\times\exp\,[iL\{\beta_j+K_z-k_z'(k_t')\}] ,\end{aligned} \tag{2·11}$$

where $\mathbf{k}_t'=\mathbf{k}_t+\mathbf{K}_t+\xi_t^{\mathbf{K}}$ with $\mathbf{K}=\mathbf{0}$ and $\mathbf{H}$. The function $\delta(\mathbf{R}', \mathbf{R}; i)$ is the Kronecker delta, being unity when $\mathbf{R}_t'$ on the exit surface satisfies the relation

$$\frac{R_t'}{\cos\varphi_K}=\frac{R_t}{\cos\varphi}-L(\nabla_t\alpha_i)_{\mathbf{K}t} . \tag{2·12}$$

Here $(\nabla_t\alpha_i)_{\mathbf{K}t}$ gives the direction of the classical energy flow of the X-ray internal field at the tie point determined by $\mathbf{k}_t$ in the initial state. Sometimes we use the vector $\mathbf{n}(\alpha_i)$ defined by

$$\mathbf{n}(\alpha_i)=-(\nabla_t\alpha_i)_{\mathbf{K}t} . \tag{2·13}$$

In a similar fashion, we can define the direction of the classical energy flow for the field in the final state $\mathbf{k}_t'$ by

$$\mathbf{n}(\beta_j)=-(\nabla_t\beta_j)_{\mathbf{K}t}' . \tag{2·14}$$

The presence of the Kronecker delta in the first term in equation (2·11) implies that the emerging position $\mathbf{R}'$ for the X-ray beam, whose scattering process is given by the first term, is exactly the same as expected in the perfect crystal; the X-ray beams scattered in the transmitted and the diffracted directions (referred to the perfect reference crystal) emerge from the exit surface at a position which is identical to the one predicted by considerations of the classical energy flow.

The presence of the Δg factors in the second term results from the atomic displacements from the ideally periodic lattice sites; it allows the scattered X-ray beam to emerge from the exit surface at different locations depending on the angular spread of the scattered direction around the transmitted and Bragg diffracted directions. According to the results in a previous paper (Kuriyama, 1968*b*), the effect of the Δg factors on scattering is produced by the displaced atoms in a limited portion of the crystal, when an incident X-ray beam is finite in its lateral dimensions. The geometrical construction for the limited portion has been discussed

in detail in the previous paper; it depends on the size of the incident beam, the direction of the energy flow, $\mathbf{n}(\alpha)$, in the initial state, the location of the observation point, $\mathbf{R}'$, and the energy flow direction, $\mathbf{n}(\beta)$, in the final state. This situation is depicted in Fig. 2. All of the atoms in the shaded portion in Fig. 2 should be taken into consideration for evaluating the Δg factors. We call this portion the diffracting domain of atoms. This domain defines an atom set $\mathscr{V}$.

The mathematical expression for the Δg factor is given in the following. The geometrical structure factor $g(\xi)$ for the crystal may be defined by

$$g(\xi)=V_c \sum_{\mathbf{l}} \exp\left[-i\xi \,.\, \mathbf{R}_{\mathbf{l}}\right] \qquad (2\cdot15)$$

where V_c is the unit-cell volume in the perfect reference crystal and $\mathbf{R}_{\mathbf{l}}$ the actual atomic position displaced by $\mathbf{u}_{\mathbf{l}}$ from the ideal lattice site $\mathbf{l}$. The Δg factor is the difference of the structure factors between the actual crystal and the perfect reference crystal with the summation extending only over the atoms in the diffracting domain:

$$\Delta g(\xi;\mathscr{V})=V_c \Sigma'\{\exp\left[-i\xi \,.\, \mathbf{R}_{\mathbf{l}}\right]-\exp\left[-i\xi \,.\, \mathbf{l}\right]\} \,. \qquad (2\cdot16)$$

It is easily seen from this equation that if the incident beam strikes a crystal portion which is perfect, and the observation point is also limited within this portion, Δg vanishes to give the scattering amplitude which is identical to that for a perfect crystal. If the beam traverses an imperfect portion, the scattering amplitude differs from that of a perfect crystal.

It is therefore an important feature of equation (2·11) that the Δg factors only convey local information about the crystal. The scattering amplitude depends on the magnitude of the local departure from perfection.

3. Structure factors for isolated imperfections

(a) A model crystal

The crystal of interest contains imperfections in such a way that each imperfection is well localized and isolated from others. The imperfection can be any type, such as a local coagulation of dislocations, a dislocation loop, an internal precipitate, a void, or a local inhomogeneous solid solution. This model certainly includes a crystal with a single dislocation, isolated impurities or vacancies. However, a continuously interlocked long-range imperfection, such as a regular dislocation array or a small angle grain boundary, is presently excluded.

In our model, the displacement of any atom from its ideal lattice site $\mathbf{l}$ is caused by just one of the im-

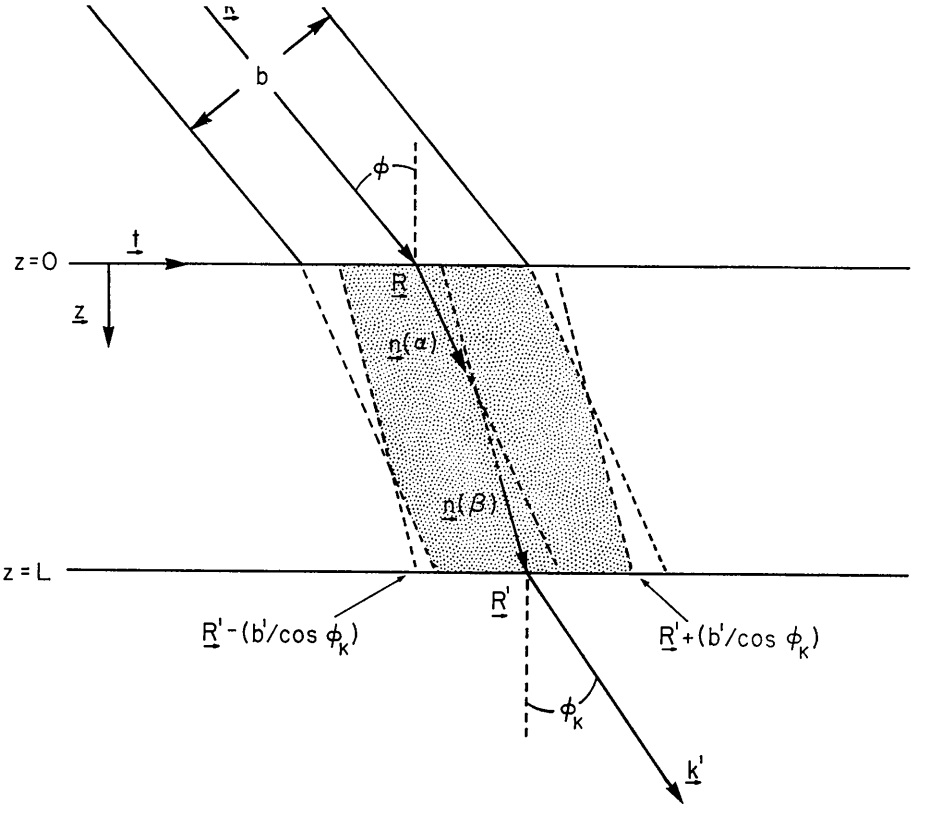

Fig. 2. Geometrical construction for the diffracting domain of atoms participating in scattering; $\mathbf{n}(\alpha)$ and $\mathbf{n}(\beta)$ are the directions of the classical energy flows in the initial and the final state, respectively. The shaded area is called the diffracting domain for the photon states of interest, which gives an atom set $\mathscr{V}$.

perfections (the condition of isolation). If the location and the designation of the imperfection are specified by $_d$ and d, respectively, then the atomic displacement at the lattice site $\mathbf{l}$ can be given by

$$\mathbf{u}_\mathbf{l} = \sum_d \mathbf{u}_\mathbf{l}^d = \mathbf{u}_\mathbf{l}^d \text{ for } l \in \mathscr{V}(d) \qquad (3\cdot1)$$

as long as the $\mathbf{l}$ belongs to the region in which the atomic displacement at a lattice site is caused by the same imperfection located at $_d$. This region may be called the effective domain of the imperfection d, and is given by an atom set $\mathscr{V}(d)$. The location $_d$ can be specified by any lattice vector within $\mathscr{V}(d)$, but, for convenience, is assumed to be the center of $\mathscr{V}(d)$. Obviously, $\mathbf{u}_\mathbf{l}^d$ vanishes unless $\mathbf{l} \in \mathscr{V}(d)$. A geometrical arrangement is illustrated in Fig. 3.

Since equation (2·16) implies that the atom contributing to the Δg factors in question must belong to $\mathscr{V}$, it is convenient to introduce another region given by the atom set $v(d)$, where $v(d)$ is the product (or intersection) of the two sets $\mathscr{V}(d)$. $\mathscr{V}$. Then the Δg factors are given by

$$\Delta g(\xi;\mathscr{V}) = V_c \sum_d \sum_{\mathbf{l}\in v(d)} \{\exp[-i\xi \,.\, \mathbf{R}_\mathbf{l}] - \exp[-i\xi \,.\, \mathbf{l}]\} \qquad (3\cdot2)$$

where d indicates the sum over the imperfection centers for which $v(d)$ is not empty. Equation (3·2) states that the scattering amplitude is given by the sum of the scattering amplitudes due to single imperfections.

(*b*) *The normal coordinate expansion*

In the normal coordinate expansion (Matsubara, 1952; Kanzaki, 1957; Yamosa & Nagamiya, 1957; Krivoglaz & Tikhonova, 1960; Krivoglaz, 1958, 1959*a*,*b*, 1960), the atomic displacement vector can be written

$$\mathbf{u}_\mathbf{l}^d = \sum_\mathbf{q} A(\mathbf{q},d) \exp[i\mathbf{q}(\mathbf{l}-{}_d)], \qquad (3\cdot3)$$

where $\mathbf{q}$ is restricted to the first Brillouin zone (the unit cell of the reciprocal lattice). The Fourier transform of the displacement vector has the property that $\mathbf{A}(\mathbf{0};d)=0$ and $\mathbf{A}^*(\mathbf{q},d)=\mathbf{A}(-\mathbf{q},d)$.

If the exponential function in (3·2) is expanded in a power series of $\xi \,.\, \mathbf{u}_\mathbf{l}$ and equation (3·3) is substituted in the series, the Δg factor is given by

$$\Delta g(\xi^K+\mathbf{K}';\mathscr{V}) = \sum_d \exp[-i\xi^K \,.\, {}_d] \sum_{n=1}^{\infty} \frac{(-i)^n}{n!} \times \sum_{\mathbf{q}1} \ldots \sum_{\mathbf{q}n} [(\xi^K+\mathbf{K}') \,.\, \mathbf{A}(\mathbf{q}_1,d)] \ldots [(\xi_\mathbf{K} + \mathbf{K}') \,.\, \mathbf{A}(\mathbf{q}_n,d)] \Delta[\xi^K - \sum_i \mathbf{q}_i; v(d)], \qquad (3\cdot4)$$

where $\zeta = \xi^K - \sum_i^n \mathbf{q}_i$ and

$$\Delta[\zeta;v(d)] = V_c \sum_{\mathbf{l}\in v(d)} \exp[-i\zeta \,.\, \mathbf{l}], \qquad (3\cdot5)$$

and $\mathbf{l}$ is measured from the center $_d$; $\xi^\mathbf{K}$ is defined by (2·1), (2·2), (2·9) and (2·10), and is a vector restricted to the first Brillouin zone; $\mathbf{K}$ takes on the value of $\mathbf{0}$ and $\mathbf{H}$, and $\mathbf{K}'$ of $\mathbf{0}$ and $\pm\mathbf{H}$. Equation (3·5) is the factor, as in the kinematical theory, that determines the effective size of the scatterer. Unlike the size effect in the kinematical theory, the X-ray absorption effect should be taken into account correctly for the present purpose. The 'mean free path' of X-rays in a single crystal may have different lengths depending on the scattered direction (and on the direction of polarization).

(*c*) *The role of absorption on the size effect*

To evaluate equation (3·5) we introduce an approximation in which the atom set $v(d)$ contains N_x, N_y and N_z atoms in the x, y, and z directions, respectively. The projected lattice constants for the perfect reference crystal are denoted by e_x, e_y and e_z. The unit-cell volume V_c is equal to $[\mathbf{e}_x\mathbf{e}_y\mathbf{e}_z]$. Then equation (3·5) reduces to

$$\Delta[\zeta;v(d)] = V_c \prod_{i=x,y,z} \sin\left(\frac{N_i+1}{2}\zeta_i e_i\right) \Big/ \sin(\tfrac{1}{2}\zeta_i e_i) \,. \qquad (3\cdot6)$$

When a crystal is in the shape of a plate as in the present problem, the x and y components of the vector ξ^K are given by real numbers, because $\mathbf{k}_t$, $\mathbf{k}'_t$ and $\mathbf{H}_t$ are real. Therefore, equation (3·6) gives the size function for the $\mathbf{x}$ and $\mathbf{y}$ directions: since N_x and N_y are large, the size function behaves like the delta function.

If the effective size $v(d)$ of the dth imperfection is small in its lateral direction compared to the lateral size of the diffracting domain, $\mathscr{V}$, (the beam size), equation (3·6) gives the imperfection range in diffraction. If the beam size is narrower than the size of the imperfection range, equation (3·6) gives the beam size effect itself.

As for the function of ζ_z in equation (3·6) some complications in evaluating it must be expected be-

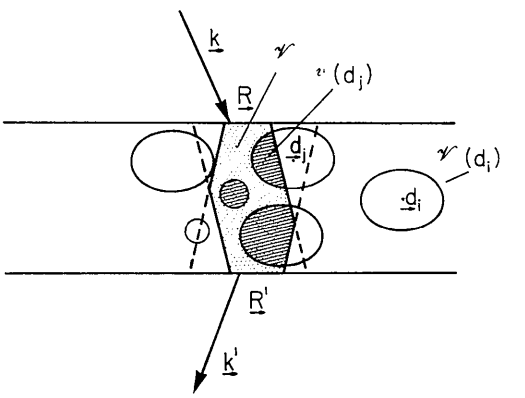

Fig. 3. Schematic illustration of the distribution of effective domains of imperfections. The vector $\mathbf{d}_i$ specifies the center position of the imperfection d_i. The loops enclose the effective domains of the imperfections which contain an atom set $\mathscr{V}(d)$. The shaded area represents the product of the two atom sets $\mathscr{V}$. $\mathscr{V}(d)=v(d)$.

cause of absorption of X-rays. The z-component, ξ_z^K becomes complex, because the solutions of the dispersion equations for the relevant states, α_i and β_j, are complex. The imaginary parts of α_i and β_j are the effective (linear) absorption coefficients in the photon state of interest. The α_i and β_j can be considered to be functions of $\mathbf{k}_t$ and $\mathbf{k}_t'$, respectively. When $\mathbf{k}_t$ or $\mathbf{k}_t'$ deviates considerably from the value for the Bragg condition, the imaginary part of $\alpha_i(\mathbf{k}_t)$ or $\beta_j(\mathbf{k}_t')$ approaches half the value of the ordinary linear absorption coefficient, μ. When $\mathbf{k}_t$ or $\mathbf{k}_t'$ satisfies the Bragg condition, the value of the imaginary part becomes either zero or μ depending on the mode of the dressed-photon (or quasi-photon) in the crystal (the mode of the dynamical fields), which is specified by i or j. We assign i or $j=1$ to the weak absorption mode, which frequently is called the anomalous transmission mode. The other mode ($i,j=2$) may be called the strong absorption mode. Fig. 4 shows the value of the imaginary parts of α_i and β_j as a function of the dimensionless variable describing the deviation from the Bragg angle for a symmetrical reflection. When the value of the imaginary parts differs considerably from the ordinary absorption coefficient, we say that the photon state is in the *dynamical diffraction range.*

Since the $\mathbf{q}$ for the displacement vector is real, the imaginary part of ζ_z is given by the imaginary part of ξ_z^K alone, regardless of the value of q_z. When $\mathrm{Im}(\xi_z^K)$ is zero, the z part of equation (3·6) becomes the ordinary size function. This occurs when either (1) the final states exactly satisfy the condition that $\mathbf{k}_t'=\mathbf{k}_t+\mathbf{K}_t$ and in addition, the mode for the final state is the same as that for the initial state: $i=j$, or (2) both the initial and the final states are outside the range of the dynamical diffraction effect.

For other states, the imaginary part of ξ_z^K has a non-zero value, either positive or negative. It is not so easy to evaluate the z part of equation (3·6) when ζ_z becomes complex. At first glance, it looks as though the function diverges when $\mathrm{Im}(\zeta_z^K)$ is positive. However, there is no divergence in the scattering amplitude. To prove this, it is better to consider the Δg factor given by (3·4) together with the factor $\exp[i\beta_j L]$ as it appears in the scattering amplitude (2·11). In equation (3·4), we have the summation over d. Therefore, the function which we shall study is given by

$$\sum_d \exp[-i\boldsymbol{\xi}^K \cdot {}_d]\Delta[\boldsymbol{\xi}^K - \sum_i \mathbf{q}_i;\nu(d)] \exp[-\mathrm{Im}(\beta_j)L] . \tag{3·7}$$

This function is written

$$V_c \sum_l \exp[-i\{\mathrm{Re}(\boldsymbol{\xi}^K)\cdot\mathbf{l}+\mathbf{q}\cdot d\}] \exp[-\mathrm{Im}(\beta_j) \times (L-l_z)] \exp[-\mathrm{Im}(\alpha_i)\cdot l_z], \tag{3·8}$$

where $\mathbf{l}$ is now measured from the entrance surface of the crystal. Since $\mathrm{Im}(\beta_j)$ and $\mathrm{Im}(\alpha_i)$ are always positive (Ashkin & Kuriyama, 1966; Kuriyama, 1967*a*) and $L-l_z$ and l_z are also positive, this function certainly converges. This is an expected consequence in the quantum mechanical formulation of any scattering theory where absorption can never be zero.

Equation (3·8) also implies that the dressed photon relating to the initial state travels inside the crystal with the absorption coefficient $\mathrm{Im}(\alpha_i)$ until it reaches the lth atom, and thereby is excited (or scattered) to be another dressed photon travelling with the absorp-

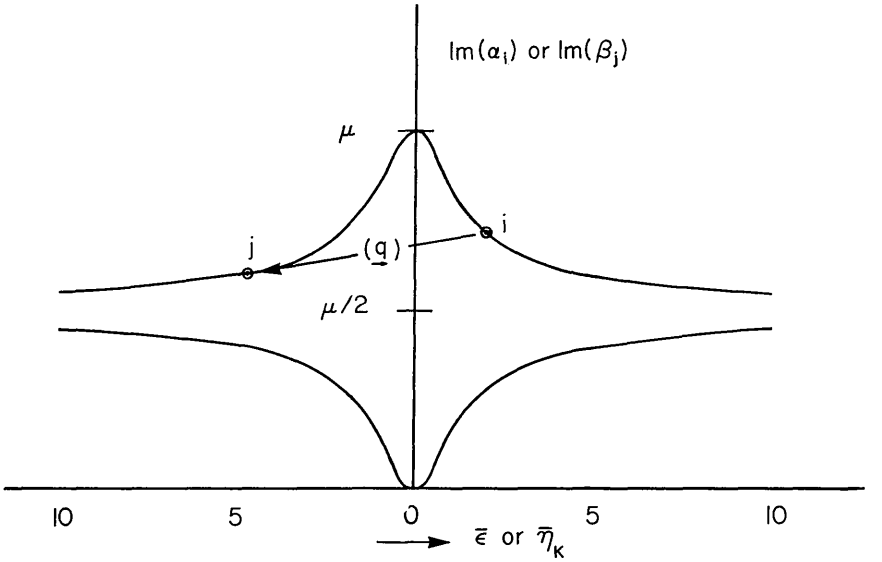

Fig. 4. The effective absorption coefficient $\mathrm{Im}(\alpha_i)$ or $\mathrm{Im}(\beta_j)$, for different modes. The mode with i or $j=1$ has a weak absorption coefficient. This is the mode for anomalous transmission; μ is the ordinary linear absorption coefficient. The quantity $\bar{\varepsilon}$ for the initial state or $\bar{\eta}_K$ for the final state is a dimensionless variable indicating a deviation from the exact Bragg condition. $\bar{\varepsilon}$ or $\bar{\eta}_K=[\mathrm{Re}\ v(\mathbf{H})v(-\mathbf{H})]^{-1/2}\times(\varepsilon$ or $\eta_{\mathbf{K}}$ in text). The arrow with (q) represents an example of a transition from the initial state i to the final state j with the momentum change, $\mathbf{q}$, due to the atomic displacements.

tion coefficient $\mathrm{Im}(\beta_j)$ all the rest of the way to the exit surface (here only the collision process of the first order is considered). The dressed photon cannot travel a longer distance than $[\mathrm{Im}(\alpha_i)]^{-1}$ or $[\mathrm{Im}(\beta_j)]^{-1}$ without appreciable absorption. If the imperfection center d is located further than $[\mathrm{Im}(\alpha_i)]^{-1}$ from the entrance surface and further than $[\mathrm{Im}(\beta_j)]^{-1}$ to the exit surface, then the atoms inside the effective domain of this imperfection $v(d)$, do not appreciably participate in the scattering process. Only the imperfection centers located favorably can scatter X-rays out of the crystal. Evaluating the z-part of equation (3·6) therefore becomes complicated, depending on the value of the $\mathrm{Im}(\alpha_i)$, $\mathrm{Im}(\beta_j)$, d and N_z.

In order to avoid this complication we introduce the following drastic simplification:

$$\left.\begin{aligned}&\mathrm{Im}(\alpha_i)l_z=\mathrm{Im}(\alpha_i)\,(l_z-d_z)+\mathrm{Im}(\alpha_i)d_z\simeq\mathrm{Im}(\alpha_i)d_z\\&\mathrm{Im}(\beta_j)\,(L-l_z)=\mathrm{Im}(\beta_j)\,(L-d_z)\\&-\mathrm{Im}(\beta_j)\,(l_z-d_z)\simeq\mathrm{Im}(\beta_j)\,(L-d_z)\end{aligned}\right\}\quad(3\cdot9)$$

where l_z belongs to the atom set $v(d)$. This is a good approximation if $N_z e_z/2$ is smaller than $[\mathrm{Im}(\alpha_i)]^{-1}$ and $[\mathrm{Im}(\beta_j)]^{-1}$. In this approximation equation (3·4) can be written

$$\Delta g(\xi^K+\mathbf{K}';\mathscr{V})=\sum_d\langle v(d)\rangle\exp\left[-i\xi^{\mathbf{K}}\cdot d\right]\times[(-i)\,(\xi^{\mathbf{K}}+\mathbf{K}')\cdot\mathbf{B}(\xi^{\mathbf{K}})-\tfrac{1}{2}M(\xi^{\mathbf{K}}+\mathbf{K}')]\,,\quad(3\cdot10)$$

where

$$\mathbf{B}(\xi^{\mathbf{K}})=\sum_{\mathbf{q}}\mathbf{A}(\mathbf{q},d)\,\langle v(d)\rangle^{-1}\Delta[\mathrm{Re}(\xi^K-\mathbf{q});v(d)]\,,\quad(3\cdot11)$$

$$M(\xi^{\mathbf{K}}+\mathbf{K}')=\sum_{\mathbf{p}}\sum_{\mathbf{q}}[(\xi^{\mathbf{K}}+\mathbf{K}')\cdot\mathbf{A}(\mathbf{p},d)]\,[(\xi^{\mathbf{K}}+\mathbf{K}')\cdot\mathbf{A}(\mathbf{q},d)]\times\langle v(d)\rangle^{-1}\Delta[\mathrm{Re}(\xi^{\mathbf{K}}-\mathbf{q});v(d)]\,,\quad(3\cdot12)$$

and $\langle v(d)\rangle$ is the volume of the atom set $v(d)$. We have ignored the products of more than two $\mathbf{A}(\mathbf{q},d)$'s.

4. Approximate expression for the scattering amplitude

The value of the real part of $\xi^{\mathbf{K}}$ is much smaller than $\mathbf{H}$ if the incident beam satisfies the Bragg condition very closely. The initial state of the photon given by the incident beam in that case certainly lies in the dynamical diffraction range. If we are interested in the scattered beams propagating in a direction almost parallel to either the transmitted or the Bragg diffracted direction, the final state of interest also lies in the dynamical diffraction range, for which the real part of $\xi^{\mathbf{K}}$ is negligibly small compared with $\mathbf{H}$. Therefore, in equation (2·11) the terms proportional to ξ and the term $M(\xi^K)$ can be neglected in comparison with the terms proportional to $\mathbf{H}$ and $M(\xi^K+\mathbf{H})$, respectively.

If the scattered beam propagates in a direction different from the above directions, the final state given by this scattered beam lies outside the dynamical diffraction range, having a larger $\xi^{\mathbf{K}}$ which may not be neglected, compared to $\mathbf{H}$. However, as is known from X-ray kinematical diffuse scattering experiments on imperfect single crystals, the diffuse scattering intensity is usually concentrated around a reciprocal lattice point. This knowledge suggests that it is reasonable to assume again that for most crystals $\mathrm{Re}(\xi)\ll H$. (Certain types of solid solution effects with super lattice formation may not justify this assumption).

The second term of the scattering amplitude (2·11) in the present approximation can be written

$$\sum_i\sum_j\langle v(d)\rangle\exp\left[-i\xi^{\mathbf{K}}\cdot d\right]\{(-i)\mathbf{H}\mathbf{B}(\xi^{\mathbf{K}})G_{ij}(+)-\tfrac{1}{2}M(\mathbf{H})G_{ij}(-)\}\,.\quad(4\cdot1)$$

We can easily calculate

$$G_{ij}(\pm)=G_{ij}(\mathbf{K}+;\xi^{\mathbf{K}})\pm G_{ij}(\mathbf{K}-;\xi^{\mathbf{K}})=v(-\mathbf{H}\delta_{\mathbf{K0}}+\mathbf{H}\delta_{\mathbf{KH}})f_{\pm}(\mathbf{K};i,j)\times F^{(2)}_{\mathbf{H}-\mathbf{K}}(\mathbf{k}_t;i)\quad(4\cdot2)$$

where

$$f_{\pm}(\mathbf{0};i,j)=(\beta_j+k'_z)\,[\Omega(\alpha_i+H_z)\pm\Omega(\beta_j+H_z)]\Delta^{-1}(\beta_j)\quad(4\cdot3)$$

$$f_{\pm}(\mathbf{K};i,j)=(\beta_j+H_z+k'_z)\,[\Omega(\beta_j)\pm\Omega(\alpha_i)]\Delta^{-1}(\beta_j)\quad(4\cdot4)$$

are effectively the extinction terms. The quantities used in (4·3) and (4·4) are defined in the Appendix.

It is interesting to note that equation (4·2) reduces to a simpler form, when β_j is equal to α_i. This is the case when the initial and final states are connected by the same mode, and the latter is scattered in the exact transmitted and Bragg diffracted directions ($\mathbf{k}'_t=\mathbf{k}_t+\mathbf{K}_t$):

$$G_{ii}(+)|_{\xi K=0}=2v(-\mathbf{H})\,\frac{\alpha_i+K_z+k'_z}{\alpha_i+k'_z}\times F^{(2)}_{\mathbf{H}}(\mathbf{k}_t;i)F^{(2)}_{\mathbf{K}}(\mathbf{k}_t;i)\quad(4\cdot5)$$

$$G_{ii}(-)|_{\xi K=0}=0\,.\quad(4\cdot6)$$

In this case, also

$$\sum_d\langle v(d)\rangle=L(ab/\cos\varphi_{\mathbf{K}})\delta(\mathbf{R}',\mathbf{R};i)\quad(4\cdot7)$$

because $\mathbf{R}'$ must satisfy the relation of equation (2·12) to give a non-vanishing unperturbed scattering amplitude.

In equations (4·3) and (4·4) it is useful to realize that $f_+(\mathbf{K};i,i)$ is almost unity and $F_-(\mathbf{K};i,i)$ is nearly zero when $j=i$, while $f_+(\mathbf{K};i,j)$ for $j\neq i$ is nearly zero and $|f_-(\mathbf{K};i,j)|$ is roughly 1, as long as ξ^K is small. From these properties of $f_{\pm}(\mathbf{K};i,j)$ we derive the approximate expression for the scattering amplitude.

We can now write

$$\langle\mathbf{k}'\mathbf{R}'|S|\mathbf{k}\mathbf{R}\rangle=S^{(1)}+S^{(2)}+S^{(3)}+S^{(4)}\,.\quad(4\cdot8)$$

The first term is the dynamical diffraction term (Kuriyama, 1967*b*) and is given by

$$S^{(1)}=T(k',k)\,(ab/\cos\varphi_K)\delta_{\mathbf{k}'_t,\mathbf{k}_t+\mathbf{H}_t}\times\sum_i\delta(\mathbf{R}',\mathbf{R};i)[1-iU(\mathbf{H})\,.\,L]\times(\alpha_i+K_z+k'_z)F^{(2)}_{\mathbf{K}}(\mathbf{k}_t;i)\times\exp\,[iL(\alpha_i+K_z-k'_z)]\,, \tag{4·9}$$

where

$$U(\mathbf{H})=(\alpha_i+k'_z)^{-1}M(\mathbf{H})v(-\mathbf{H})F^{(2)}_{\mathbf{H}}(\mathbf{k}_t;i)\,. \tag{4·10}$$

If $U(\mathbf{H})$ is zero as expected in a perfect crystal, equation (4·9) becomes identical with the result obtained in the dynamical theory.

The second term $S^{(2)}$ implies that there is an additional effect due to the imperfections on the dynamical term. This second term is, in its interaction process, equivalent to the third term, which arises from kinematical scattering of the dynamically diffracted X-rays and is due to the imperfections. The third term is given first as follows:

$$S^{(3)}=T(k',k)\sum_{i\neq j}W(\mathbf{H})F^{(2)}_{\mathbf{H}-\mathbf{K}}(\mathbf{k}_t;i)\times\exp\,[i\{\mathrm{Re}(\beta_j)+K_z-k'_z\}]\,, \tag{4·11}$$

where

$$W(\mathbf{H})=\sum_d\langle v(d)\rangle\mathbf{H}\mathbf{B}(\mathbf{q})v(-\mathbf{H}\delta_{\mathbf{KO}}+\mathbf{H}\delta_{\mathbf{KH}})\times f_-(\mathbf{K};i,j)\times\exp\,[-i\mathbf{q}\,.\,d]\times\exp\,[-\mathrm{Im}(\beta_j)\,(L-d_z)]\exp\,[-\mathrm{Im}(\alpha_i)d_z] \tag{4·12}$$

with $\mathbf{q}_t=\mathbf{k}'_t-\mathbf{k}_t-\mathbf{K}_t$ and $q_z=\mathrm{Re}(\beta_j-\alpha_i)$. The $S^{(3)}$ term results from the transition of the dressed photon in the initial mode i to the differing mode $j(j\neq i)$. This transition is accompanied by the phase shift, $\mathrm{Re}(\beta_j-\alpha_i)$, and the relevant change in the effective absorption coefficient. It should be noted that this term $S^{(3)}$ is *not* proportional to $F^{(2)}_{\mathbf{K}}(\mathbf{k}_t;i)$ (as is the dynamical term $S^{(1)}$), *but* to the dynamical field function $F^{(2)}_{\mathbf{H}-\mathbf{K}}(\mathbf{k}_t;i)$. Since the third term gives non-vanishing scattering amplitudes in directions other than in the transmitted and the Bragg diffracted directions, this $S^{(3)}$ term essentially gives the 'diffuse' scattering effect around the Laue spots. This remark applies equally to scattering around the 'zero' Laue spot, that is produced by the angularly undeviated beam. The total intensity from this 'diffuse' scattering ($S^{(3)}$) can easily exceed the intensity due to the dynamical term, and depends strongly on the crystal thickness and the locations of the imperfections. The second term $S^{(2)}$ is a special case of $S^{(3)}$ and is given by

$$S^{(2)}=S^{(3)}(\mathbf{k}'_z=\mathbf{k}_t+\mathbf{K}_t;\beta_j=\alpha_i)\,. \tag{4·13}$$

It corresponds to diffuse scattering angularly coincident with the intensity arising from term $S^{(1)}$ and cannot be independently observed.

The fourth term is the correction to the third in the present approximation. This term $S^{(4)}$ results from the interaction, in which two different Fourier transforms of the atomic displacement vector, $\mathbf{A}(\mathbf{q},d)$ and $\mathbf{A}(\mathbf{q}',d)$ are involved. A process involving $\mathbf{q}$ and $-\mathbf{q}$ can be treated more rigorously. Kuriyama & Miyakawa (1969) have used the corrected Bragg diffracted propagators for X-ray diffraction from a piezoelectrically vibrating crystal to include the process involving $\mathbf{q}$ and $-\mathbf{q}$. According to their results, the dynamical field functions $F^{(2)}_{\mathbf{K}}(\mathbf{k}_t;i)$ should be corrected by the exact narrowing of the dynamical rocking curve width (the extinction distance). In the present approximation, the fourth term appears mainly because we have not corrected the dynamical field functions as initially employed in $S^{(1)}$, $S^{(2)}$ and $S^{(3)}$.

Finally, we consider the final state $\mathbf{k}'_t$ when it is far outside the dynamical diffraction region. Then, ξ cannot be ignored as compared to H. For such $\mathbf{k}'_t$, we can easily prove that $F^{(1)}_{\mathbf{H}}(\mathbf{k}'_t,j)\simeq 0$, and that $F^{(1)}_{\mathbf{O}}(\mathbf{k}'_t;j)$ approaches either zero or 1, depending upon which way $\mathbf{k}'_t$ deviates from the Bragg condition. Therefore, from equations (2·6) and (2·7), the scattering amplitude close to the Bragg diffracted direction becomes proportional to $(\xi+\mathbf{H})B(\xi)F^{(2)}_{\mathbf{O}}(\mathbf{k}_t;i)$, exactly as expected from the kinematical diffuse scattering theory.

Results and discussion

(*a*) *Isolated imperfections*

In a linear theory of lattice imperfections, the atomic displacement is given by a superposition of the displacements due to individual imperfections. Since a casual study of X-ray diffraction shows that the scattering amplitude is a complicated function of the atomic displacements, one cannot generally say that the scattering amplitude is given by a superposition of the scattering amplitudes from the crystal having single imperfections. It is, however, self-evident and observed from topographic images by X-ray diffraction that only the imperfections under a certain region irradiated by an incident X-ray beam can be revealed in these images as though they were independent of other imperfections which were not irradiated by the incident beam.

In a previous study (Kuriyama, 1968*b*) and the present paper, it has, in fact, been shown that the scattering amplitude is expressed by the local behavior of the imperfections under the incident beam. Furthermore, it has now been shown that this scattering amplitude can be described by a superposition of the effects due to single imperfections as long as the imperfections are isolated mutually though irradiated simultaneously.

(*b*) *The expansion approximation used in evaluating* Δg

In evaluating the Δg factors, we have used a Taylor expansion in a power series of $\xi\,.\,\mathbf{u}$. As the convergence of this series is usually poor, this approximation certainly is not good. If the exact coordinates of the displaced atoms could be given, the numerical calculation of the Δg factors would be performed. However, this is not practical at present. Instead, one should introduce models of general types of imperfections.

The quantitative scattering data are then tested against the quality of agreement with the calculated intensity using the model. The quantitative atomic displacement parameters can be obtained from the models. Finally these parameters can be compared to other information and theories of crystal imperfection. The present paper only aims at an understanding of basic processes of diffraction, especially those processes in which dynamical diffraction is dominant.

As we have seen theoretically, the atomic displacements appear in the scattering amplitude as a kind of geometrical factor, while the diffraction processes are involved in the dynamical field functions, $F_{\mathbf{K}}^{(1)}(\mathbf{k}_t';j)$ and $F_{\mathbf{K}}^{(2)}(\mathbf{k}_t;i)$. In other words, $G_{ij}(\mathbf{K}+;\xi^{\mathbf{K}})$ and $G_{ij}(\mathbf{K}-;\xi^{\mathbf{K}})$ functions in (2·11) contain the complete processes of the dynamical interaction, and the Δg factors are coefficients determining the weight of each dynamical process. In this sense, the present expansion approximation does not change the description of the dynamical interaction. We may therefore say that this treatment is a convenient approximation to study the basic processes of diffraction.

The present expansion approximation becomes a good one when (*a*) the magnitudes of the atomic displacements are very small (strain of less than one per cent) and/or (*b*) the imperfection covers a long range but is characterized by a slow rate of change of strain with distance, although the magnitude of the strain may exceed one per cent. The latter condition can be generalized a little further, specifically to include solid solution inhomogeneities in which the imperfection consists in a change of scattering power in a specific cell in addition to an atomic displacement. The expansion approximation is good whenever the Fourier transform $A(\mathbf{q},d)$ of the atomic displacements approaches zero quickly as $\mathbf{q}$ increases. Fortunately, these two cases represent most situations studied in current X-ray experiments and theories.

(*c*) *The dynamical diffraction term* $S^{(1)}$

The $S^{(1)}$ term becomes identical to the result obtained from the dynamical theory when all atoms rest at perfect crystal sites. The change in the dynamical diffraction due to the crystal imperfections is described by $S^{(1)}$, and the term itself is caused purely by the dynamical interactions in the imperfect crystal.

The decrease in the Borrmann (anomalous) transmission is therefore contained in this term. A white (lower intensity) image or shadow of a defect appears on a black, anomalously transmitted background, when the X-rays encounter a defect region. The disruption of the Borrmann transmitted beam is caused by a change in the effective absorption coefficient due to the local distortions.

The $S^{(1)}$ term also explains the narrowing of the dynamical diffraction range resulting from the imperfections. If one could make a measurement of the rocking curve width (or extinction distance) for the $S^{(1)}$ term alone, the width would be smaller than that for a perfect crystal. This conclusion implies that it is difficult for a crystal to maintain the dynamical diffraction effect as the imperfections increase.

We can demonstrate the disruption of the Borrmann effect and the narrowing of the dynamical diffraction range explicitly for a symmetrical reflection condition in the Laue geometry. As in a previous paper (Kuriyama, 1967*b*) we write the factor $1-iU(\mathbf{H})\,.\,L$ in equation (4·9) as $\exp[-iU(\mathbf{H})L]$ and combine it with the other factor $\exp[i\alpha_i L]$. Then the dynamical diffraction term can be written

$$S^{(1)}=[\text{Dyn. Amp.}]\exp[i\{\alpha_i-U(\mathbf{H})\}\,.\,L]\,, \quad (5\cdot1)$$

where [Dyn. Amp.] is the dynamical amplitude of the transmitted or Bragg diffracted X-ray beam obtained in the dynamical theory for a perfect crystal. For a symmetrical reflection, one obtains

$$\begin{aligned}\alpha_i-U(\mathbf{H})\simeq{}& k\cos\theta_B+\frac{1}{2}\frac{\mathrm{Re}\{v(\mathbf{0})\}}{k\cos\theta_B}+\frac{1}{2}\frac{1}{k\cos\theta_B}\\ &\times\left[\varepsilon\pm\sqrt{\varepsilon^2+\{1-M(\mathbf{H})\}\,\mathrm{Re}\{v(\mathbf{H})v(-\mathbf{H})\}}\right]\\ &+i\frac{1}{2}\frac{\mathrm{Im}\{v(\mathbf{0})\}}{k\cos\theta_B}\left[1\pm\frac{1}{2}\frac{\{1-M(\mathbf{H})\}}{\sqrt{\varepsilon^2+\mathrm{Re}\{v(H)v(-H)\}}}\right.\\ &\left.\times\frac{\mathrm{Im}\{v(\mathbf{H})v(-\mathbf{H})\}}{\mathrm{Im}\{v(\mathbf{0})\}}\right], \quad (5\cdot2)\end{aligned}$$

where θ_B is the Bragg angle, $\mathrm{Im}\{v(\mathbf{0})\}/k$ is the ordinary linear absorption coefficient μ, and $2\varepsilon=\mathbf{k}_t^2-(\mathbf{k}_t+\mathbf{H}_t)^2$. The real part of $\alpha_i-U(\mathbf{H})$ is the phase shift due to the dynamical diffraction effect and involves the factor $[1-M(\mathbf{H})]$ in the square root term. The imaginary part also contains the term $[1-M(\mathbf{H})]$, which indicates the change in the effective absorption coefficient.

Furthermore, if we approximate $1-M(\mathbf{H})$ by $\exp[-M(\mathbf{H})]$, equation (5·2) suggests that the factor $v(\mathbf{H})v(-\mathbf{H})$ is, in effect, modified by $\exp[-M(H)]$, being similar in form to the thermal Debye–Waller correction. The real part indicates that the rocking curve width for $S^{(1)}$ is now $v(\mathbf{H})v(-\mathbf{H})\exp[-M(\mathbf{H})]$, implying the narrowing of the dynamical diffraction range (Kikuta & Kohra, 1966). The imaginary part indicates that the change in the effective absorption coefficient is caused by the factor $\mathrm{Im}\{v(\mathbf{H})\}\exp[-M(\mathbf{H})]$, instead of $\mathrm{Im}\{v(\mathbf{H})\}$ in the perfect crystal. These effects have been explained by Dederichs (1967) and Kuriyama (1967*b*) when defects are statistically distributed throughout the crystal. This term also contains the Pendellösung effect in an imperfect crystal.

(*d*) *The second term* $S^{(2)}$

The second term, like the third term, is the effect of kinematical scattering of the dynamically diffracted X-rays due to the imperfections. This effect weakens the contrast of white images produced by the $S^{(1)}$ term as the crystal distortion increases, because the X-ray

intensity due to the $S^{(2)}$ term increases in proportion to the effective volume of the imperfection domains and the Fourier transforms of the atomic displacement vectors. The $S^{(2)}$ term is, to some extent, responsible for the non-uniform background in the anomalous transmission (diffraction) beams, and has the effect of partial occultation of the $S^{(1)}$ amplitude.

(*e*) *The effect of the third term* $S^{(3)}$

This term plays essentially the same role as the $S^{(2)}$ term. However, the complicated images in topographs may be caused mainly by this term, because the X-rays scattered by the imperfections emerge from the crystal exit surface with a certain spatial divergence. This spatial (angular) divergence arises naturally from the above treatment even though no such divergence is postulated for the incoming beam. A geometric interpretation is given in Fig. 5.

The crystal is irradiated by a beam thought of as sweeping across the surface in the plane of the Figure while maintaining the Bragg angle θ_B for a plane whose reciprocal lattice vector is chosen parallel to **t**. For beam position 1 striking a defect, X-rays can emerge at any position **R′** between the limits indicated on the Figure (Kuriyama, 1968*b*). The contribution of this beam 1 to the $S^{(1)}$ curve takes into account the Borrmann disruption of the defect. The dotted curve in Fig. 5(*a*) illustrates that contribution as compared with any other beam position (beam 2 in Fig. 5) that fails to strike a defect. Fig. 5(*b*) illustrates the contribution of the $|S^{(2)}+S^{(3)}|^2$ term. Beam 2 does not contribute any intensity, but beam 1 does. Apart from the geometrical factor due to the atomic displacements, this intensity distribution as a function of **R′** is essentially given by $|f_-(\mathbf{K};i,j)F^{(2)}_{\mathbf{H}-\mathbf{K}}(\mathbf{k}_t,i)|^2$. Fig. 5(*c*) combines all the observable intensities from the swept-beam experiment. In this case we have considered a single isolated defect. In addition, in a practical experiment the incoming beam would have a finite dimension perpendicular to the plane of Fig. 5. Whereas the contributions to the $S^{(1)}$ term would show no angular spread, the defect scatter of Fig. 5(*b*) would have a

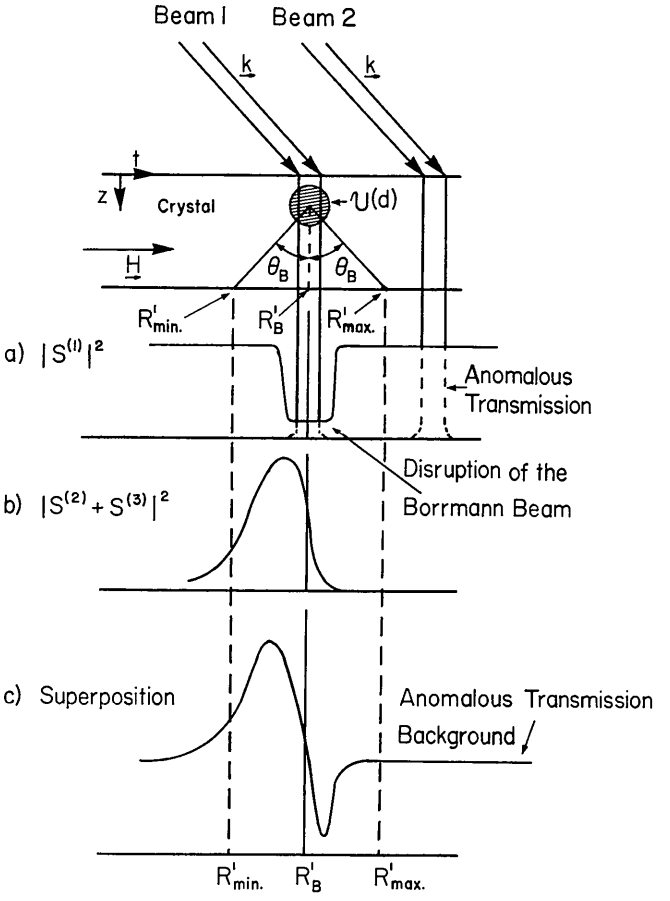

Fig. 5. Explanation of black-white contrast image in topographs for symmetrical Laue geometry. Beam 1 is the beam portion striking an imperfect portion of the crystal, whereas Beam 2 strikes a perfect portion. Solid curve in (*a*) represents the anomalous transmission (diffraction) intensity as the function of the position of the incident beam. Curve (*b*) represents the scattering due to the imperfect domain $v(d)$ in the Bragg diffracted beam. The resultant curve is given by the curve (*c*). $R'_{\min}$ and $R'_{\max}$ determine the range over which X-rays scattered by the defect may emerge from the crystal.

small angular spread out of the plane of the Figure. In some accurate experiments on a highly inhomogeneous crystal it might be necessary to take such divergence into account. However, most of the black-white contrast images could be explained semi-quantitatively by this kind of intensity distribution shown in Fig. 5(*c*).

As we mentioned in § 4, whereas the first term is proportional to $F_{\mathbf{K}}^{(2)}(\mathbf{k}_t;i)$, the $S^{(2)}$ and $S^{(3)}$ terms are proportional to the dynamical field function $F_{\mathbf{H}-\mathbf{K}}^{(2)}(\mathbf{k}_t;i)$. This implies that the X-rays are scattered in a direction nearly parallel to the Bragg diffracted direction with the amplitude proportional to the dynamical field function $F_{0}^{(2)}(\mathbf{k}_t;i)$ which is related to the dynamical scattering in the transmitted direction, and vice versa. The function $F_{\mathbf{H}}^{(2)}(\mathbf{k}_t;i)$ is well localized within the dynamical diffraction region, while $F_{0}^{(2)}(\mathbf{k}_t;i)$ tends to approach a free photon behavior. The effect of the defect on diffraction therefore is more prominent in the Bragg diffracted direction than in the transmitted direction.

(*f*) *The thickness of the crystal and the depth of imperfection centers*

Next we consider the effect of the crystal thickness on the images and their contrast. For a thin crystal ($\mu L<1$) the $S^{(1)}$ term does not give a prominent anomalous transmission effect, but shows almost the same effect as in the kinematical scattering, because both modes ($i=1$ and 2) are equally effective. However, there is a possibility of seeing a faint anomalous transmission effect in an exceptionally perfect region of the crystal image. The other terms give the kinematical diffuse scattering or line broadening, because the dressed photon of the initial mode α_i can reach all the imperfections under the incident beam and is thereby scattered into the final mode β_j, which can travel through the crystal without appreciable absorption: $L-d_z \ll [\mathrm{Im}(\beta_j)]^{-1}$ and $d_z \ll [\mathrm{Im}(\alpha_i)]^{-1}$ in equation (4·12). Therefore, we would expect to see black images of larger size than the incident beam around defects, and probably a faint undiffused anomalous transmission trace of the size of the beam from the perfect portion of the crystal.

For a crystal of intermediate thickness, the $S^{(1)}$ term shows an anomalous transmission effect through a perfect portion of the crystal and white images at the site of imperfections because of the effect described in (*c*). The other terms give black images and the black-white contrast images described in (*d*). Generally the images are expected to be complicated because the depth of the imperfections affects the resultant intensity distribution [see equation (4·12)]. Image contrast becomes better in this range of thickness.

For a thick crystal ($\mu L>10$), the $S^{(1)}$ term gives white images of defects with good contrast on the background due to the otherwise anomalously transmitted (or diffracted) beam. The other terms ($S^{(2)}+S^{(3)}$) show little effect on the background, except for the imperfections located near the exit crystal surface. This result may account for the often surprising contrast from surface imperfections such as scratch marks.

(*g*) *The limiting case of a highly imperfect crystal*

When the crystal is highly imperfect, the scattering amplitude is dominated by the $S^{(2)}$ and $S^{(3)}$ terms. However, the amplitude does not exceed the value expected from the kinematical theory, because the Δg factors never exceed the crystal volume or the volume of the diffracting domain.

(*h*) *Additional comments*

When the diffracting domain is constructed at an observation point $\mathbf{R}'$, one must take into account two tie points for different modes, which are called conjugate points. Detailed discussions on this subject have been made in a previous paper (Kuriyama, 1968*b*).

For topography in high resolution, the size of the incident beam should be considered more carefully. In order to obtain topographs of high spatial resolution, an incident beam of extremely small size is needed. Then the momentum divergence in the incident wave packet becomes wider than the range of dynamical diffraction. In the zero order approximation, we may obtain the correct result by integrating the present scattering amplitude over $\mathbf{k}_t$.

The author wishes to thank Mr H.S.Peiser and Dr A.W.Ruff for their helpful discussions.

APPENDIX

The dynamical field functions

For a single Bragg reflection, the momentum $\mathbf{k}$ of the photon in the initial state approximately satisfies the Bragg condition $|\mathbf{k}|=|\mathbf{k}+\mathbf{H}|$. Then, the following function of a vector variable $\mathbf{p}$ becomes useful:

$$\det m(\mathbf{p})=\Omega(\mathbf{p})\Omega(\mathbf{p}+\mathbf{H})-v(\mathbf{H})v(-\mathbf{H}) \qquad (A\text{-}1)$$

where

$$\Omega(\mathbf{p})=\mathbf{p}^2-k^2-v(\mathbf{0})\,. \qquad (A\text{-}2)$$

The possible modes, α_i, of the dressed photon created by the incoming photon and the crystal electrons are determined by the dispersion equation for the initial state ($\mathbf{k}_t$ given):

$$[\det m(\mathbf{p})]_{\mathbf{p}_t=\mathbf{k}_t,p_z=\alpha_i}=0 \text{ for } \alpha_i\,. \qquad (A\text{-}3)$$

The dynamical field functions for this state are given by

$$F_{-\mathbf{H}}^{(2)}(\mathbf{k}_t;i)=0 \qquad (A\text{-}4)$$

$$F_{0}^{(2)}(\mathbf{k}_t;i)=(\alpha_i+k_z)\Omega(\alpha_i+H_z)\,[\Delta(\alpha_i)]^{-1} \qquad (A\text{-}5)$$

$$F_{\mathbf{H}}^{(2)}(\mathbf{k}_t;i)=(\alpha_i+k_z)v(+\mathbf{H})\,[\Delta(\alpha_i)]^{-1}\,, \qquad (A\text{-}6)$$

where

$$\Omega(\alpha_i+H_z)=[\Omega(\mathbf{p})]_{\mathbf{p}_t=\mathbf{k}_t+\mathbf{H}_t,p_z=\alpha_i+H_z} \qquad (A\text{-}7)$$

and

$$\Delta(\alpha_i)=\left[\frac{\partial}{\partial p_z}\det m(\mathbf{p})\right]_{\mathbf{p}_t=\mathbf{k}_t,p_z=\alpha_i}\,. \qquad (A\text{-}8)$$

In a similar fashion, the possible modes of the dressed photon creating the outgoing photon in the final state are determined by the dispersion equations for the final state of interest. For a single Bragg reflection the two major propagation directions of the outgoing photons are significant in their final states: the state having $\mathbf{k}'$ almost parallel to $\mathbf{k}$ (the transmitted direction) and the state having $\mathbf{k}'$ almost parallel to $\mathbf{k}+\mathbf{H}$ (the Bragg diffracted direction).

For the final state in which $\mathbf{k}'\sim\mathbf{k}$ the modes β_j^0, which is equal to β_j in (2·10), are given by the dispersion equation

$$[\det m(\mathbf{p})]_{\mathbf{p}_t=\mathbf{k}'_t,p_z=\beta_j}=0\,, \qquad (A\text{-}9)$$

and give the dynamical field functions

$$F_{-\mathbf{H}}^{(1)}(\mathbf{k}'_t;j)=(\beta_j+k'_z)v(-\mathbf{H})\,[\Delta(\beta_j)]^{-1} \qquad (A\text{-}10)$$

$$F_{0}^{(1)}(\mathbf{k}'_t;j)=(\beta_j+k'_z)\Omega(\beta_j+H_z)\,[\Delta(\beta_j)]^{-1} \qquad (A\text{-}11)$$

$$F_{-\mathbf{H}}^{(1)}(\mathbf{k}'_t;j)=0\,, \qquad (A\text{-}12)$$

where

$$\Omega(\beta_j+H_z)=[\Omega(\mathbf{p})]_{\mathbf{p}_t=\mathbf{k}'_t+\mathbf{H}_t,p_z=\beta_j+H_z} \qquad (A\text{-}13)$$

and

$$\Delta(\beta_j)=\left[\frac{\partial}{\partial p_z}\det m(\mathbf{p})\right]_{\mathbf{p}_t=\mathbf{k}'_t,p_z=\beta_j}\,. \qquad (A\text{-}14)$$

For the final state in which $\mathbf{k}'$ is almost equal to $\mathbf{k}'+\mathbf{H}$, it is convenient to use the variables $\bar{\mathbf{k}}'=\mathbf{k}'-\mathbf{H}$ and β_j [defined in (2·10)] instead of $\mathbf{k}'$ and $\boldsymbol{\beta}_j^H$. Then, β_j is determined by

$$[\det m(\mathbf{p})]_{\mathbf{p}_t=\bar{\mathbf{k}}',p_z=\beta_j}=0\,. \qquad (A\text{-}15)$$

The dynamical field functions are given by

$$F_{-\mathbf{H}}^{(1)}(\mathbf{k}'_t;j)=0 \qquad (A\text{-}16)$$

$$F_{0}^{(1)}(\mathbf{k}'_t;j)=(\beta_j+H_z+k'_z)\Omega(\beta_j)\,[\Delta(\beta_j)]^{-1} \qquad (A\text{-}17)$$

$$F_{\mathbf{H}}^{(1)}(\mathbf{k}'_t;j)=(\beta_j+H_z+k'_z)v(+\mathbf{H})\times[\Delta(\beta_j)]^{-1}\,, \qquad (A\text{-}18)$$

where

$$\Omega(\beta_j)=[\Omega(\mathbf{p})]_{\mathbf{p}_t=\bar{\mathbf{k}}'_t=\mathbf{k}'_t-\mathbf{H}_t,p_z=\beta_j} \qquad (A\text{-}19)$$

and

$$\Delta(\beta_j)=\left[\frac{\partial}{\partial p_z}\det m(\mathbf{p})\right]_{\mathbf{p}_t=\bar{\mathbf{k}}'_t,p_z=\beta_j}\,. \qquad (A\text{-}20)$$

In evaluating these functions it would be convenient to use, instead of $\mathbf{k}_t$ and $\mathbf{k}'_t$, the variables indicating the deviation from the exact Bragg condition. In particular, it is extremely difficult to determine $\mathbf{k}_t$ and $\mathbf{k}'_t$ with a great degree of accuracy on the absolute scale in experiments. However, one can measure the deviation of the scattering angle for the relevant state on a relative scale from the exact Bragg angle θ_B. We denote the angle deviations for the initial state and for the two final states by $\delta\varphi$, $\delta\varphi_0$, and $\delta\varphi_{\mathbf{H}}$, respectively. The Bragg angle θ_B is defined by

$$2|\mathbf{Q}|\sin\theta_B=|\mathbf{H}|\,, \qquad (A\text{-}21)$$

where

$$|Q|^2=k^2+v(\mathbf{0})\,. \qquad (A\text{-}22)$$

Then the variables for the deviation are given by

$$\varepsilon=|\mathbf{Q}|^2\sin 2\theta_B\,.\,\delta\varphi \qquad (A\text{-}23)$$

and

$$\eta_{\mathbf{K}}=|\mathbf{Q}|^2\sin 2\theta_B\,.\,\delta\varphi_{\mathbf{K}} \qquad (A\text{-}24)$$

with $\mathbf{K}=\mathbf{0}$ and $\mathbf{H}$ depending on which final state is of interest. In terms of these variables, the quantities needed for the initial state are given by

$$\alpha_t=Q_z+\frac{1}{2(Q_z+H_z)}\times\left[\varepsilon\pm\sqrt{\varepsilon^2+\left(\frac{Q_z+H_z}{Q_z}\right)v(-\mathbf{H})v(\mathbf{H})}\right] \qquad (A\text{-}25)$$

$$\Omega(\alpha_t)=\frac{Q_z}{Q_z+H_z}\times\left[\varepsilon\pm\sqrt{\varepsilon^2+\left(\frac{Q_z+H_z}{Q_z}\right)v(-\mathbf{H})v(\mathbf{H})}\right] \qquad (A\text{-}26)$$

$$\Omega(\alpha_t+H_z)=-\varepsilon\pm\sqrt{\varepsilon^2+\left(\frac{Q_z+H_z}{Q_z}\right)v(-\mathbf{H})v(\mathbf{H})}\,, \qquad (A\text{-}27)$$

where Q_z is the z-component of $\mathbf{Q}$. For the final state, β_j and Ω's are obtained by replacing α_t and ε by β_j and $\eta_{\mathbf{K}}$, respectively.

It is obvious from these calculations that the dynamical field functions for the initial state, $F_{\mathbf{K}}^{(2)}(\mathbf{k}_t;i)$, become identical to the electric field intensity of radiation outside the crystal in the dynamical theory.

References

ASHKIN, M. & KURIYAMA, M. (1966). *J. Phys. Soc. Japan*, **21**, 1549.

BORRMANN, G. (1941). *Phys. Z.* **42**, 157.

BORRMANN, G. (1950). *Z. Physik*, **127**, 297.

DEDERICHS, P. H. (1967). *Phys. Stat. Sol.* **23**, 377.

KANZAKI, H. (1957). *J. Phys. Chem. Solids*, **2**, 24, 107.

KIKUTA, S. & KOHRA, K. (1966). *J. Phys. Soc. Japan*, **21**, 1449.

KRIVOGLAZ, M. A. (1958). *J. Expl. Theor. Phys. USSR*, **33**, 204.

KRIVOGLAZ, M. A. (1959*a*). *Fiz. Metal. Metalloved.* **7**, 650.

KRIVOGLAZ, M. A. (1959*b*). *Fiz. Metal. Metalloved.* **8**, 648.

KRIVOGLAZ, M. A. (1960). *Fiz. Metal. Metalloved.* **10**, 169.

KRIVOGLAZ, M. A. & TIKHONOVA, Y. A. (1960). *Ukr. fiz. zhurn.* **5**, 174.

KURIYAMA, M. (1967*a*). *J. Phys. Soc. Japan*, **23**, 1369.

KURIYAMA, M. (1967*b*). *Phys. Stat. Sol.* **24**, 743.

KURIYAMA, M. (1968*a*). *J. Appl. Phys.* **39**, 2162.

KURIYAMA, M. (1968*b*). *J. Phys. Soc. Japan*, **25**, 846.

KURIYAMA, M. & MIYAKAWA, T. (1969). *J. Appl. Phys.* **40**, 1967.

MATSUBARA, T. (1952). *J. Phys. Soc. Japan*, **7**, 270.

YOMOSA, S. & NAGAMIYA, T. (1957). *J. Phys. Soc. Japan*, **12**, 610.